BOREAL ENVIRONMENT RESEARCH 21: 427–444
ISSN 1239-6095 (print) ISSN 1797-2469 (online)

Helsinki 4 February 2016

Radiation measurements at the Pallas-Sodankylä Global Atmosphere Watch station — diurnal and seasonal cycles of ultraviolet, global and photosynthetically-active radiation

Kaisa Lakkala[1)2)], Anna Jaros[1)], Mika Aurela[3)], Juha-Pekka Tuovinen[3)], Rigel Kivi[1)], Hanne Suokanerva[1)], Juha M. Karhu[1)] and Tuomas Laurila[3)]

[1)] *Finnish Meteorological Institute, Arctic Research Centre, Tähteläntie 62, FI-99600 Sodankylä, Finland*
[2)] *Finnish Meteorological Institute, Climate Research, P.O. Box 503, FI-00101 Helsinki, Finland*
[3)] *Finnish Meteorological Institute, Atmospheric Composition Research, P.O. Box 503, FI-00101 Helsinki, Finland*

Received 5 June 2015, final version received 15 Dec. 2015, accepted 18 Dec. 2015

Lakkala K., Jaros A., Aurela M., Tuovinen J.-P., Kivi R., Suokanerva H., Karhu J.M. & Laurila T. 2016: Radiation measurements at the Pallas-Sodankylä Global Atmosphere Watch station — diurnal and seasonal cycles of ultraviolet, global and photosynthetically-active radiation. *Boreal Env. Res.* 21: 427–444.

We present time series of solar ultraviolet radiation (UVR), global radiation, and photosynthetically-active radiation (PAR) measurements from the Pallas-Sodankylä Global Atmosphere Watch (GAW) station at Sodankylä for the period 1990–2013. Measurements were performed both in an open area and in the surrounding boreal forest, which had a total leaf area index of 3.6. We present a method to homogenize multifilter radiometer UV time series. Using this method, the relative mean differences between the multifilter radiometer and the reference spectroradiometer were 5% for UVB and erythemally-weighted dose rates, for all sky conditions and solar zenith angles (SZA) smaller than 60° during the period 2008–2012. Our results show that daily doses measured in the forest were four times smaller than those measured in the nearby open area. Maximum UVB (280–320 nm) and UVA (320–400 nm) daily doses of 75.0 kJ m^{-2} and 1.74 MJ m^{-2}, respectively, were measured during the period of multifilter radiometer measurements, 2002–2012. The maximum daily sum of global radiation during the years 2000–2010 was 31.4 MJ m^{-2}, measured in 2010. The maximum PAR during 2000–2012 was 1830 μmol m^{-2} s^{-1}, measured in 2000. For the entire period of spectral UV measurements, 1990–2013, a maximum UV index of 6 was measured in 2011 and 2013.

Introduction

The Arctic and subarctic ecosystems include species that live on the border of their area of distribution and are sensitive to even small changes in climatic conditions. In previous years and decades, stratospheric ozone depletion in spring was observed at Sodankylä (Kyrö *et al.* 1992, Von der Gathen *et al.* 1995, Kivi *et al.* 2007, Manney *et al.* 2011), which led to an increase in UV radiation (UVR) reaching the ground. This can have large effects on nature and humans (Young *et al.* 1993), as nature is not well-prepared to cope with the increased solar radiation levels occurring after a long and dark winter. After the discovery of stratospheric

Editor in charge of this article: Veli-Matti Kerminen

ozone depletion in the Antarctic (Farman *et al*. 1985), international regulations, i.e. the Montreal Protocol, have restricted the use of ozone-depleting substances. Nowadays, the recovery of the stratospheric ozone layer is suggested to have started (Andrady *et al*. 2009, WMO 2011, 2014) and future climate scenarios suggest an ozone "super recovery", where total ozone amounts at high Arctic latitudes will be even higher than before the ozone depletion (Eyring *et al*. 2013). This will lead to less UV radiation reaching the ground; e.g., the WMO (2011) and Fountoulakis *et al*. (2014) suggest over 10% decreases in UV radiation by the second half of the 21st century.

Future UV scenarios strongly depend on changes in other factors affecting UVR as well. Changes in ground albedo, aerosols and cloudiness can either mask or strengthen the effect of changes in total ozone. At high latitudes, changes in ground albedo and cloudiness are predicted due to global warming (IPCC 2013). However, the rate and magnitude of such changes are still unknown, and high-quality observations are needed, in order to detect the first signs of any changes.

In this paper, we present time series of shortwave solar radiation affecting the Earth's ecosystems as measured at the Pallas-Sodankylä GAW station in Finland, i.e., UVR, photosynthetically-active radiation (PAR) and global radiation (R_g). We also include the total ozone time series, as total ozone is one of the key factors affecting the solar UVR reaching the ground (Arola *et al*. 2003, Lakkala *et al*. 2003). We study inter-annual changes in the time series, and show typical diurnal and annual cycles of the measured quantities.

Material

The radiation measurements were carried out at the Finnish Meteorological Institute Arctic Research Centre (FMI-ARC) at Sodankylä (67.37°N, 23.63°E). Together with the Pallas Atmospheric Research Station, the Centre forms the Pallas-Sodankylä GAW station. The station is located in Finnish Lapland, in a boreal environment. From the point of view of stratospheric meteorology, the site can be classified as an Arctic site with periods of Arctic ozone depletion in spring.

The areas surrounding the station are covered by peatlands and boreal coniferous forest. The river Kitinen runs to the west of the station. Snow covers the ground from October to April, and the sun is below the horizon for several days in December, whereas it shines for 24 hours around mid-summer. Minimum temperatures can reach –40 °C, and maximum ones +30 °C.

Measurements were performed at four different locations in the local area of the Arctic Research Centre (Table 1). All these places are located within 500 m of each other. The spectral UVR and total ozone measurements were performed from the roof of the sounding station, denoted hereafter as "roof", representing an open area. Multichannel radiometer measurements were performed in the forest and on peatland as well as from the roof. The PAR was also measured from a micrometeorological mast at a height of 45 m. The global radiation was measured both from the micrometeorological mast (at 45 m) and from the radiation tower (at 16 m).

Table 1. The location, instrumentation and time periods of the UVR, PAR, R_g and total ozone measurements used in this study.

Quantity	Location	Instrument	Period
Spectral UV	Roof	Brewer MKII	1990–2013
Multichannel UV, PAR	Roof	NILU-UV	2002–2013
Multichannel UV, PAR	Peatland	NILU-UV	2002–2006
Multichannel UV, PAR	Forest	NILU-UV	2002–2011
PAR	Micromet. mast	LI-190SZ	2000–2012
Total ozone	Roof	Brewer MKII	1988–2013
Global radiation	Radiation tower	CM11	2000–2010

UVR and total ozone measurements

Spectral UVR and total ozone measurements

Spectral UV measurements were performed using Brewer spectroradiometers. The homogeneous time series started in 1990, and consists of measurements using a Mark II type Brewer spectroradiometer (Brewer #037, SCI-TEC, Canada). A second Brewer spectroradiometer, a Mark III (Brewer #214, Kipp & Zonen, The Netherlands) was set up at the Sodankylä station in 2012. Here, we analyzed data from Brewer #037 for consistency of the time series.

The Mark II type Brewer measures in the wavelength range 290–325 nm every half an hour. The wavelength resolution is 0.5 nm, with a full width at half maximum (FWHM) of 0.56 nm; one scan takes about 3 minutes. The Brewer has a flat Teflon® diffuser and a single monochromator. The quality control (QC) and the quality assurance (QA) of the measurements, as well as the entire data processing procedure, are described in detail in Lakkala *et al*. (2008). Spectral data are corrected for stray light, dark counts, temperature dependence, cosine error and wavelength shifts. As part of the QA, the spectroradiometer participates in international comparisons, and comparisons with radiative transfer calculations and broadband radiometer measurements are also made. The European portable reference spectroradiometer QASUME from the Physikalisch-Meteorogisches Observatorium Davos (Gröbner and Sperfeld 2005), World Radiation Center (PMOD/WRC), regularly visits the site, and comparison results for 2003–2014 show an agreement of better than 6%.

The irradiance scale of UV measurements is traceable to the Aalto University, which is the national standards laboratory for optical quantities in Finland (Kübarsepp *et al*. 2000), where the primary standard of the FMI is annually calibrated. The calibration scale was transferred to the whole time series after 1990, which makes this time series one of the longest homogeneous spectral UV time series measured in the Arctic.

Originally, Brewer spectroradiometers were built to measure total ozone. At Sodankylä, total ozone measurements were started in 1988. Total ozone measurements are traceable to the Brewer triad in Toronto, Canada, via a travelling reference Brewer, and to the WMO/GAW Regional Brewer Calibration Center for Europe (RBCC-E) in Tenerife, Spain. The spectroradiometer has participated in several international total ozone measurement comparisons, and shows an agreement of 1%–2% with the reference instrument (Karppinen *et al*. 2014). Garane *et al*. 2006 estimated the combined uncertainty of the spectral UV measurements of the Brewer #005 at Thessaloniki to be ±6.5% at 305 nm and ±5% at 320 nm. These uncertainties can be considered to be a good estimate of those of the Brewer #037 at Sodankylä, as both instruments are single Brewers having similar error sources, and the data processing includes similar correction procedures.

Multichannel UVR measurements

Multichannel UVR measurements were performed with a NILU-UV multi-filter radiometer, type NILU-UV6T, manufactured by Innovation NILU AS, Norway. The measurements were started in 2002, in order to serve the Finnish Ultraviolet Irradiation Centre (FUVIRC). One NILU-UV was set up in a peatland field and a second one in the forest. The forest measurements were conducted in a 50–130-year-old Scots pine forest under a canopy, having a total leaf area index of 3.6 (Thum *et al*. 2007) and average height of 12 m. During the first years, the instruments measured only during the field experiment season, but in 2008 the peatland instrument was moved onto the roof of the station, and has since measured all year around. The last forest measurements were from 2011. In total, five different NILU-UV instruments were used for measurements at the station (Table 2).

The NILU-UV radiometer has five channels in the UV wavelength region, with centre wavelengths at 305, 312, 320, 340 and 380 nm, and bandwidths of around 10 nm at FWHM. Using the measurements of these channels, UVB, UVA, erythemally-weighted (McKinlay and Diffey 1987) and plant-damage-weighted (Caldwell *et al*. 1986) dose rates can be calculated using the method described in Dahlback (1996).

Total ozone and cloud information can also be retrieved from the measurements. A sixth channel measures the PAR in the visible 400–700 nm wavelength region. The radiometer has a flat Teflon® diffuser, silicon detectors, and bandpass filters and is temperature stabilized to 40 °C. The data are stored as one-minute averages. The characteristics of the instrument are described in more detail in Høiskar *et al*. (2003), where they reported that the cosine corrected erythemally weighted UV dose rates agreed with those from a Bentham spectroradiometer to 0.99 ± 0.03.

Global radiation

Global radiation (shortwave solar radiation, R_g) was measured by the Kipp & Zonen CM11 thermopile pyranometers. The CM11 measures solar radiation in the wavelength range 305–2800 nm. Kratzenberg *et al*. (2006) determined that the combined uncertainty for a CM11 measurement of R_g of 800 W m^{-2} was 1.9%. Wang *et al*. (2012) showed that a well-maintained pyranometer of the World Meteorological Organization (WMO) secondary standard, e.g., the Kipp & Zonen CM11, has an uncertainty of 2%–5%. R_g was measured from the radiation tower and from the micrometeorological mast, which were situated within 500 m from each other. The measurements from the radiation tower were the primary measurements, started in 1971 (Kivi *et al*. 1999). When the CO_2 and H_2O flux measurements were started at Sodankylä in 2000, a second instrument was installed on the micrometeorological mast. The primary instrument is replaced every third year with a calibrated unit, whose calibration is performed at the Swedish Meteorological and Hydrological Institute (SMHI) in Norrköping. The operation of the second sensor is compared with the primary one and may be recalibrated against that during the post-processing of the data. In addition to the incoming solar radiation, reflected radiation was also measured with a CM11, providing information on the surface albedo at both locations.

Table 2. The serial numbers, operational period and location of the NILU-UV multifilter radiometers at Sodankylä.

Serial number	Operational period	Location
13	2007–2008	Roof
31	2002–2006	Peatland
32	2002–	Forest, roof since 2011
102	2007–2008	Roof, albedo measurements
131	2008–	Roof

PAR measurements

PAR, which represents the part of the solar radiation that plants can utilize (400–700 nm), was measured by the NILU-UV radiometer's sixth channel and by a radiometer LI-190SZ (LI-COR, Inc.). The photon flux density was measured over the visible-light spectral range (400–700 nm). The unit used by the NILU-UV PAR was E m^{-2} s^{-1}, whereas the PAR measured with the LI-190SZ was presented in the corresponding SI unit of μmol m^{-2} s^{-1} expressing how many micromoles of photons are measured at a surface unit per unit time. For the NILU-UV, the original factory calibration, based on a lamp traceable to the National Institute of Standards and Technology (NIST), was used during the whole measurement period. The changes in the responsivity of the channel were monitored by performing regular lamp tests (Fig. 1). More than two lamps were used in order to distinguish possible lamp drifts from the drift of the responsivity of the radiometer. The results showed that for the NILU no. 131, the responsivity of the PAR channel was stable within 2% over the period 2008–2013.

The incoming and reflected PAR have been measured from the station's micrometeorological mast since 2000 by the LI-190SZ quantum sensor. The LI-190SZ sensors were used with their factory calibration, any change in the calibration being quantified using the primary global radiation instrument. The PAR measurements were traceable to the NIST; following the manufacturer of the LI-190SZ, the uncertainty due to the absolute calibration of the instrument was ±5% (Table 3). In this study, we calculated the PAR time series measured with both the NILU-UV and the LI-190SZ instruments, but only the LI-190SZ data were analyzed further, as the uncertainties of the NILU-UV instrument were not evaluated.

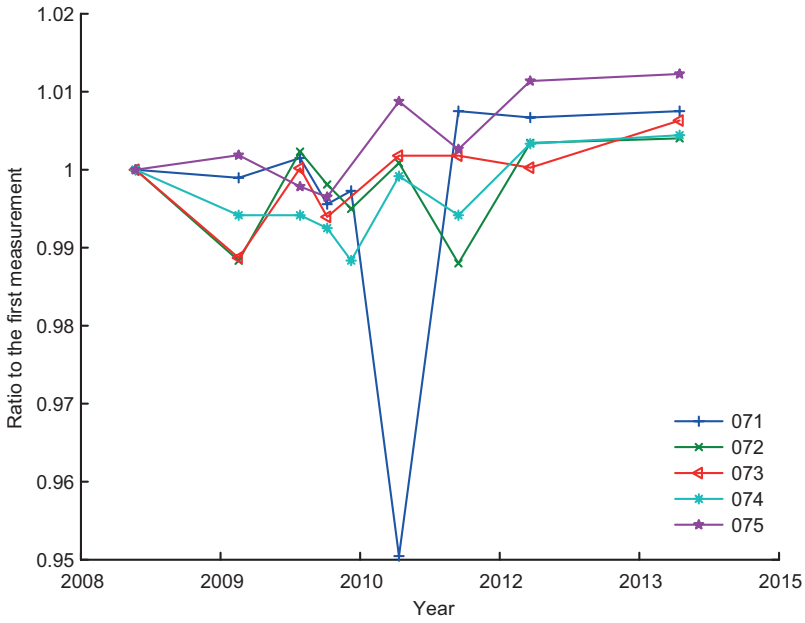

Fig. 1. Stability measurements of the PAR channel of the NILU-UV no. 131. Lamps no. 071–075 were used. Each measurement was compared with the first measurement. An example of an erroneous measurement can be seen in the case of lamp no. 071 in 2010.

Methods

Time series

For each measured parameter, homogenized time series were derived from the measurements. We studied each month separately, in order to take into account the effect of seasonal changes in factors affecting radiation conditions at the ground, e.g., solar zenith angle, Sun–Earth distance, ground albedo, cloudiness, aerosols and total ozone.

We assessed the shortwave radiation climate at Sodankylä by calculating monthly mean diurnal cycles of PAR and R_g. The diurnal cycles were calculated from half-hour averages. The yearly cycles of erythemally-weighted, UVB and UVA daily doses were calculated from the NILU-UV measurements. Monthly means of four UV products, PAR, R_g and total ozone (TO) were also calculated. As unequally distributed data gaps may generate systematic errors on the monthly statistics of solar radiation, we calculated these statistics only for months that had data from more than 25 days. The total ozone monthly means were calculated for months, which had more than 16 measurement days, i.e., data from March–September/October.

The biological effect of UV radiation is often estimated by calculating the biologically-effective irradiance

$$E_{\mathrm{eff}} = \int_{\lambda_1}^{\lambda_2} E(\lambda) S(\lambda) d(\lambda), \qquad (1)$$

where $S(\lambda)$ is the biological action spectrum, λ is the measured wavelength and E is the

Table 3. The specifications of the LI-190SZ instrument as provided by the manufacturer, LI-COR, Inc. (www.licor.com).

Absolute calibration	±5% traceable to the National Institute of Standards and Technology (NIST)
Sensitivity	Typical 8 μA per 1000 μmol s^{-1} m^{-2}
Linearity	Maximum deviation of 1% up to 10 000 μmol s^{-1} m^{-2}
Stability	Typically < ±2% change over a 1 year period
Response time	10 μs
Temperature dependence	0.15% per °C, maximum
Cosine correction	Cosine corrected up to 80° angle of incidence
Azimuth	< ±1% error over 360° at 45° elevation

measured irradiance. The biologically-weighted or non-weighted spectral irradiances, integrated over the whole spectral interval (Eq. 1) are also called dose rates. In this work, we used the CIE (Commission International de l'Éclairage) erythema (McKinlay and Diffey 1987) and the plant damage (Caldwell *et al*. 1986*)* action spectra. We also calculated the biologically-effective daily dose

$$H_{\mathrm{eff}} = \int_{t_1}^{t_2} E_{\mathrm{eff}}\, dt, \qquad (2)$$

where t is time. Daily doses of erythemally-weighted (ERY) and plant-damage-weighted (PLANT) UVR, UVB (280–320 nm) and UVA (320–400 nm) were calculated for both open area and forest environments. The ratio of erythemally-weighted UV and UVA (320–400 nm) daily doses was calculated, as changes in total ozone amounts should be seen in the ERY/UVA ratio. This is due to the UV absorbing effect of ozone, which is stronger at UVB than at UVA wavelengths.

Nowadays, especially for public information, the use of the UV index (UVI) has become popular. The UVI is calculated by multiplying the erythemally-weighted UV irradiance (Eq. 1), expressed in W m^{-2}, by 40 (WMO 1997). In this work, UVI time series were derived from the Brewer spectroradiometer measurements.

Quality assurance of NILU-UV measurements

The NILU-UV radiometers were initially calibrated by the manufacturer, the irradiance scale being traceable to the National Institute of Standards and Technology (NIST) via the laboratory of SP, the Swedish testing and Research Institute (Johnsen *et al*. 2002). The method of calibration is described in Dahlback (1996), and is based on comparisons of NILU-UV measurements with measurements of a spectroradiometer and with radiative transfer calculations. As part of the QA, we performed regular lamp tests and comparisons with our Brewer spectroradiometer's measurements. As described in Lakkala *et al*. (2005), the sensitivity of the channels of the NILU-UV tend to drift over the years and the influence of the drift should be corrected. This can be done using three different methods: (1) The instrument can be recalibrated using the method described in Dahlback (1996), in which the spectral response function of the channels are taken into account, and the measurements are calibrated against a spectroradiometer. (2) Lakkala *et al*. (2005) introduced a simple method for instruments having the same spectral response functions. A scaling coefficient was determined for each channel by comparing the NILU-UV with a travelling reference. This method cannot be used for instruments having different spectral responsivities, as spectral changes in solar UVR would not be detected correctly. (3) Diaz *et al*. (2005) introduced a method based on calibration against a travelling reference using multiregression methodology, which takes into account total ozone and SZA. This minimized the errors due to differences in spectral response functions between the reference and site radiometers. Johnsen *et al*. (2002) also implemented comparisons with a travelling reference and correction for the SZA and total ozone dependency.

The spectroradiometer at Sodankylä did not cover the entire spectral range of the NILU-UV, which meant, that an absolute calibration, following the method of Dahlback (1996), was not possible at the site. However, the UV products measured with the NILU-UV, i.e., dose rates, could be scaled to the measurements of the spectroradiometer in order to obtain homogenized time series. Even though our Brewer did not measure irradiances at wavelengths longer than 325 nm, UV dose rates (Eq. 1) were calculated over the whole UV wavelength interval 290–400 nm. This was possible as the standard Brewer UV-processing algorithm includes a simple method of generating the irradiance at wavelengths longer than 325 nm: the measurement at 324 nm is used to scale a pre-defined spectrum at 324–400 nm. As the pre-defined spectrum is not a real measurement, we did not consider it suitable for absolute calibration, but the integrals over a specified wavelength range (dose rates) are useful in comparisons.

We scaled four different UV products calculated from the NILU-UV measurements to the corresponding products calculated from the Brewer spectral measurements:

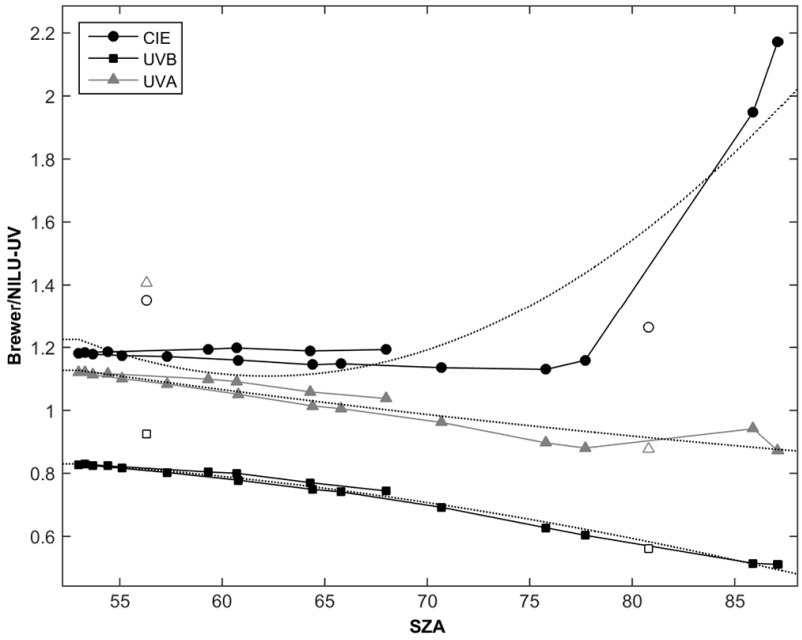

Fig. 2. Ratios of erythemally-weighted (CIE), UVB and UVA dose rates calculated from Brewer measurements and NILU-UV measurements as a function of solar zenith angle (SZA) on 14 Aug. 2011. The open symbols denote measurements made during changing cloud conditions and therefore excluded from the analysis. The dotted lines are polynomial fits.

1. The UVB dose rate (DR_{UVB}, λ_1 = 280 nm, λ_2 = 320 nm and $S(\lambda) = 1$ in Eq. 1).
2. The UVA dose rate (DR_{UVA}, λ_1 = 320 nm, λ_2 = 400 nm and $S(\lambda) = 1$ in Eq. 1).
3. The erythemally-weighted UV dose rate (DR_{ERY}, λ_1 = 290 nm, λ_2 = 400 nm and $S(\lambda)$ is the erythema action spectrum (McKinlay and Diffey 1987) in Eq. 1).
4. The plant damage dose rate (DR_{plant}, λ_1 = 290 nm, λ_2 = 400 nm and $S(\lambda)$ is the plant damage action spectrum (Caldwell *et al*. 1986) in Eq. 1).

The scaling involved four steps:

1. Calculating the ratio c of NILU-UV and Brewer measurements for the above-mentioned four UV products.
2. Plotting these ratios as a function of SZA.
3. Fitting polynomials to the plot of c *versus* SZA, separately for every month and year.
4. Scaleing the UV products calculated from the NILU-UV measurements with the polynomial fit functions. There is a different set of functions for every month.

These steps are explained in more detail below.

The ratio c was calculated for the four UV products (DR_{UVB}, DR_{UVA}, DR_{ERY}, DR_{plant}) calculated from the NILU-UV (NILU) and Brewer (Brewer) measurements:

$$c = \frac{\text{Brewer}\left(DR_i\right)}{\text{NILU}\left(DR_i\right)}, \quad (3)$$

where i denotes UVB, UVA, ERY or plant. The ratio was calculated and plotted versus SZA for each Brewer measurement (Fig. 2).

A solar zenith angle dependency was clearly seen in the ratios c. This may be for several reasons: e.g., (a) even though the Brewer measurements were corrected for the cosine error, the uncertainties in the measurements do increase towards a higher SZA; (b) at high SZA, the stray light problem of single Brewers also becomes more dominant (Bais *et al*. 1996); (c) the retrieval of dose rates from multifilter measurements includes the SZA dependency and correction (Dahlback 1996), but most probably some error still remains; (d) the NILU-UV measurements were not corrected for cosine error, whose effect is most pronounced at high SZA (Høiskar *et al*. 2003).

As the Brewer is a scanning instrument, and takes around 3 minutes to measure the entire spectrum, the cloud cover has time to change

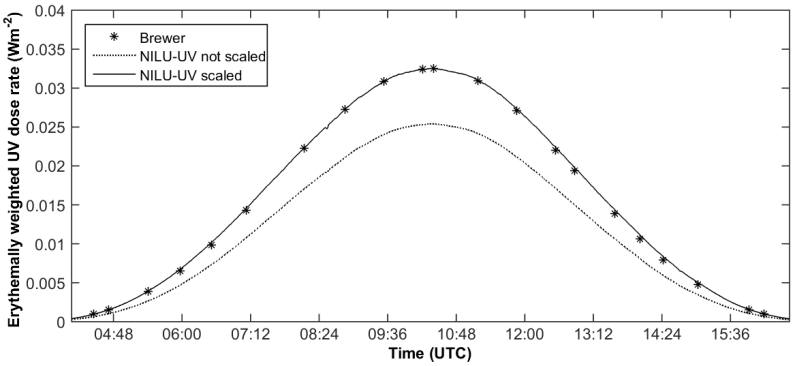

Fig. 3. Erythemally-weighted NILU-UV dose rates scaled using the correction function, as well as uncorrected measurements, compared to the Brewer measurements on 25 Mar. 2010. The day had clear sky conditions.

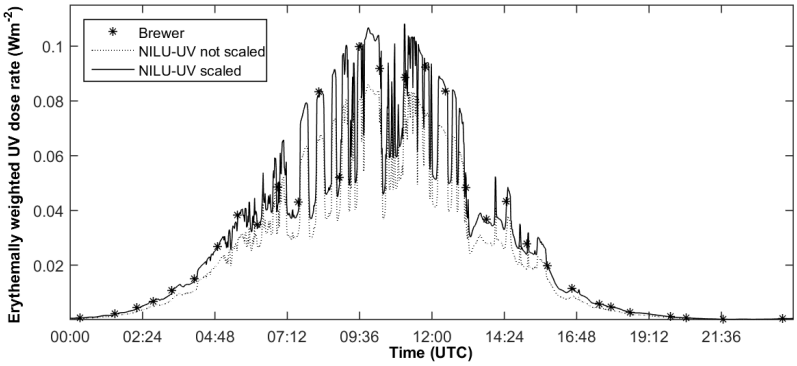

Fig. 4. Erythemally-weighted NILU-UV dose rates scaled using the correction function, as well as uncorrected measurements, compared to the Brewer measurements on 6 Jun. 2010. The day had conditions of variable cloudiness.

during the scan. The NILU-UV instrument monitors more rapid cloud changes, as it calculates a one-minute average dose rate. This led to differences, when comparing the NILU-UV dose rates with those measured by the Brewer, even if the average of three successive NILU-UV measurements was used. The comparisons affected by changing cloudiness could be recognized when plotting the ratios c, as the ratios of erroneous measurements did not follow the regular SZA dependency (Fig. 2).

In order to exclude seasonal variations in the atmospheric conditions affecting UV radiation measured at the ground, such as the natural seasonal variation of total ozone and aerosols, as well as changes in ground albedo due to snow, we calculated the ratios c for each month separately. As much as possible, we used measurements made during uniform cloud conditions. We calculated polynomial fits to the ratios c for each UV product and month separately (Fig. 2). The polynomial fits were weighted towards the smallest SZA.

We used the so-obtained polynomial fits as an SZA-dependent correction function to scale the NILU-UV dose rates (Figs. 3 and 4) for SZA ≤ 82°. For SZAs higher than 82°, the correction was kept constant, equal to that at an SZA of 82°. This was due to the high uncertainty of Brewer measurements at such SZAs. The analysis showed that, using the correction function, the relative mean differences between the Brewer and NILU-UV for the period 2008–2012 were reduced by more than 10% and 20% for erythemally-weighted and UVB dose rates, respectively, at SZAs smaller than 60° (Table 4). The corresponding reductions in the relative differences for UVA and plant-damage-weighted dose rates were 5% and 7%, respectively. The final QA of the NILU-UV measurements was carried out by comparing daily doses with those calculated from the Brewer measurements. If the relative difference was more than 20%, the measurements of the NILU-UV were flagged. The measurements made on the peatland and from the roof of the station were combined in order to get longer

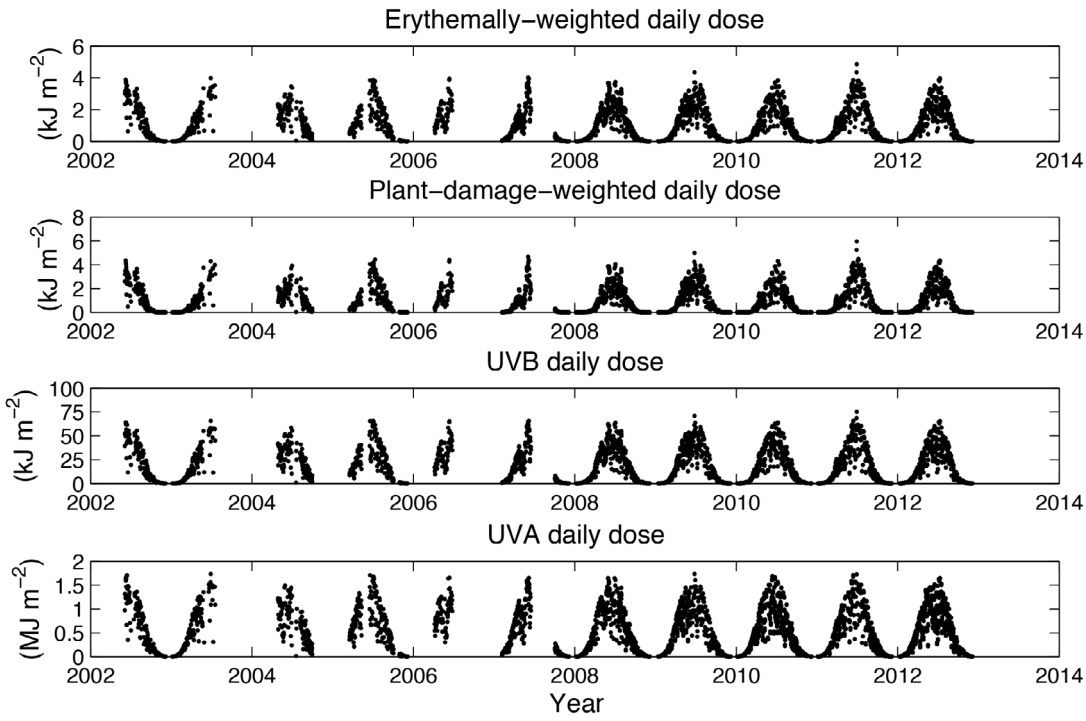

Fig. 5. Erythemally and plant-damage-weighted UVR, UVB and UVA daily doses calculated from the NILU-UV measurements performed on the peatland (prior to 2007) and from the roof of the observatory (after 2007) at Sodankylä in 2002–2012.

UV time series. The distance between these sites was only 500 m and both sites represent an open area with similar regional albedo. Thus no significant differences in the downwelling UV irradiance were expected between the sites.

Results and discussion

UVR daily doses

Erythemally and plant-damage-weighted, UVB and UVA daily dose time series were calculated for both an open area and the forest (Figs. 5 and 6, Table 5). For the open area, the maximum erythemally-weighted, plant-damage-weighted and UVB daily doses of 4.86 kJ m^{-2}, 5.96 kJ m^{-2} and 75.2 kJ m^{-2}, respectively, were recorded in June 2011. The maximum measured UVA daily dose, 1.74 MJ m^{-2}, occured in June 2009.

In the forest, the UVR was about four times less intense than in the open area. Maximum erythemally-weighted, plant-damage-weighted and UVB daily doses of 1.28 kJ m^{-2}, 1.57 kJ m^{-2} and 19.6 kJ m^{-2}, respectively, were recorded in June 2011. The maximum measured UVA daily dose, 467 kJ m^{-2} occured in June 2009.

The maximum UV indices, UVI 6, were measured in the summers of 2011 and 2013 (Fig. 7). The most important reason for these high UV values was the meteorological conditions prevailing during these days: ozone-poor

Table 4. The average relative difference and standard deviation (± 1σ) between the Brewer and NILU-UV's (no. 131) corrected and uncorrected values of erythemally-weighted (ERY), UVB and UVA dose rates, and dose rates weighted with the plant damage action spectrum (PLANT).

	ERY	UVB	UVA	PLANT
Uncorrected	0.161 ± 0.055	0.252 ± 0.099	0.172 ± 0.102	0.110 ± 0.042
Corrected	0.048 ± 0.048	0.046 ± 0.054	0.118 ± 0.102	0.038 ± 0.038

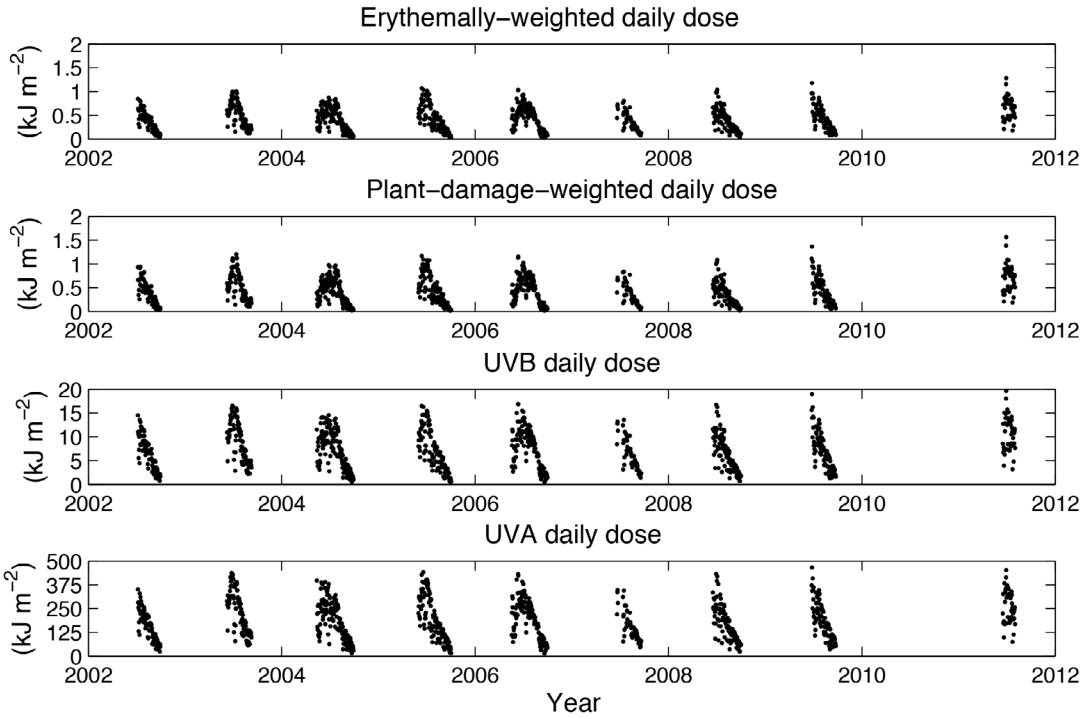

Fig. 6. Erythemally and plant-damage-weighted UVR, UVB and UVA daily doses measured with the NILU-UV in the forest at Sodankylä in 2002–2011.

mid-latitude air mass was located over Finland, an area of high pressure occurred, and the sky was cloudless. Also, especially in 2011, the influence of the previous springtime ozone depletion could still be seen. For example Karpechko *et al*. (2013) showed the connection between severe springtime ozone depletion and high summer UV irradiances in the Arctic.

Diurnal and annual cycles of PAR, R_g and UVR

A maximum measured PAR of 1830 μmol m^{-2} s^{-1} occurred in June 2000, while a maximum R_g daily

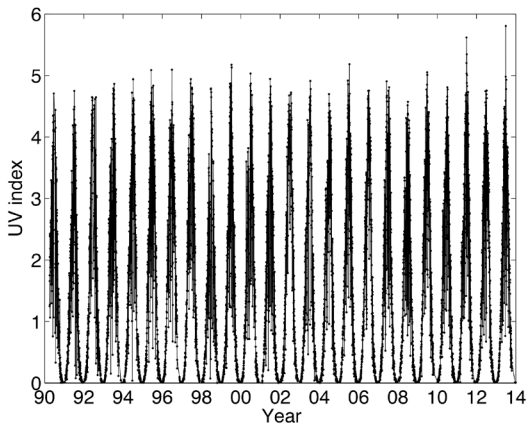

Fig. 7. Daily maximum UV indices measured with the Brewer spectroradiometer in 1990–2013.

Table 5. Maximum daily doses of erythemally (ERY) and plant-damage (PLANT) weighted UVR, UVB and UVA.

	Open area	Forest
ERY UVR	4.86 kJ m^{-2} (30 Jun. 2011)	1.28 kJ m^{-2} (30 Jun. 2011)
PLANT UVR	5.96 kJ m^{-2} (30 Jun. 2011)	1.57 kJ m^{-2} (30 Jun. 2011)
UVB	75.2 kJ m^{-2} (30 Jun. 2011)	19.6 kJ m^{-2} (30 Jun. 2011)
UVA	1.74 MJ m^{-2} (26 Jun. 2009)	467 kJ m^{-2} (26 Jun. 2009)

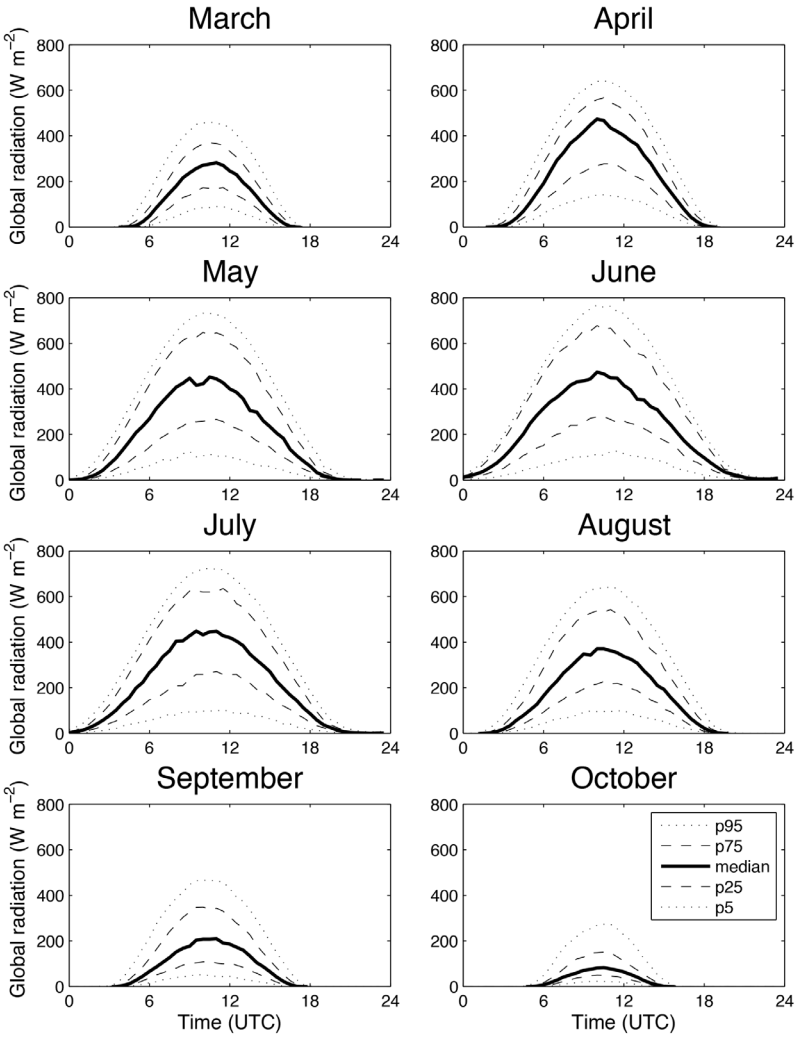

Fig. 8. Average diurnal cycle of global radiation measured on the radiation tower at Sodankylä in 2000–2010. The 5th, 25th, 50th (median), 75th and 95th percentiles are plotted.

sum of 31.44 MJ m^{-2} took place in June 2010. We calculated the median of diurnal cycles of R_g (Fig. 8), measured on the radiation tower during the years 2000–2010, and PAR (Fig. 9), measured with the LI-190SZ instrument in March–October during the years 2000–2012. Diurnal cycles were also calculated from the NILU-UV radiometer PAR measurements for the period 2008–2013. Throughout the diurnal cycle, the medians calculated from the LI-190SZ data were higher than those calculated from the NILU-UV measurements. The reasons may lie in differences in calibration, the studied period or in the instrument horizon, as the LI-190SZ measurements are performed on the micrometeorological mast and the NILU-UV measurements from the roof of the station. Over the same period, i.e., 2009–2012 for both instruments, the average difference in June was around 20% at midday.

For both PAR and R_g, the highest daily values varied little between April and July, even though SZAs are smaller at midday in June and July than in April and May. The reason may be that there was still snow on the ground in April and May, which increased the radiation reflected from the ground. Also high pressure weather conditions are common in April and May, resulting in low cloudiness, whereas clouds are frequent in June and July. However, the morning/evening radiation is higher in the summer than in the spring.

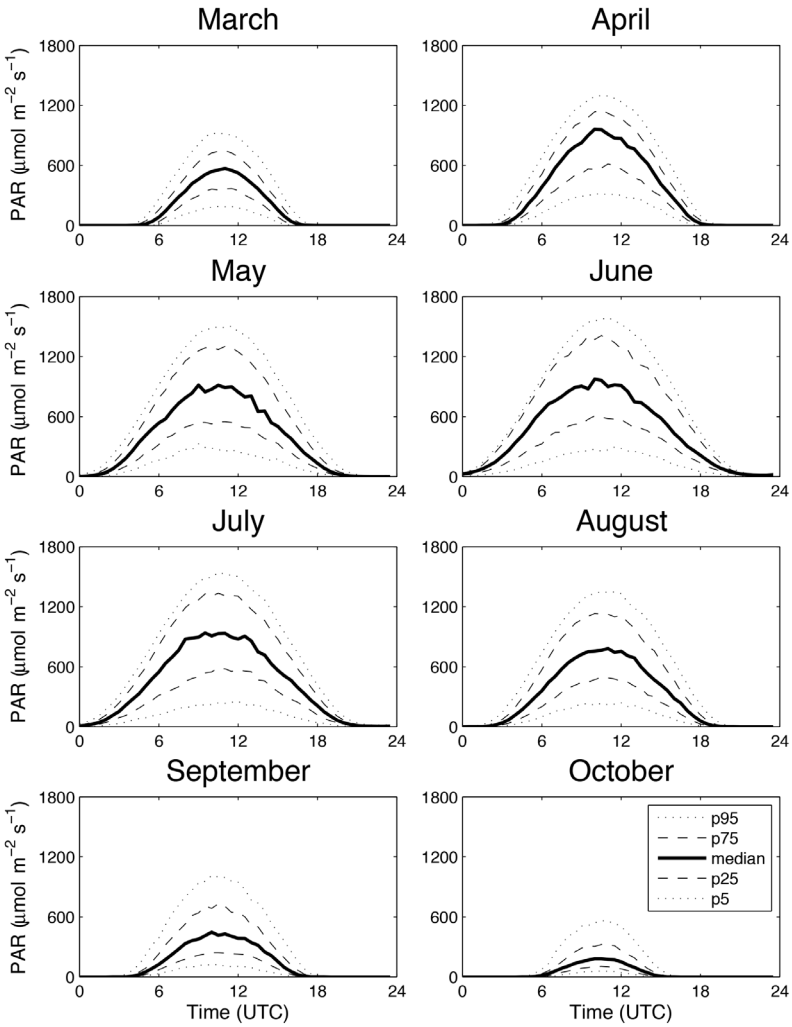

Fig. 9. Average diurnal cycle of photosynthetically-active radiation (PAR) measured with the LI-190SZ on the micrometeorological mast at Sodankylä in 2000–2012. The, 5th, 25th, 50th (median), 75th and 95th percentiles are plotted.

Making use of the time series measured with the NILU-UV during the period 2002–2012, we calculated daily means for each day of the year for the erythemally-weighted, UVB and UVA daily doses (Fig. 10). The effect of the spring-time snow cover is seen in April–May as enhanced UV doses (Meinander *et al*. 2008). For June and July, the daily means are rather similar, with a higher standard deviation in late June/July.

Inter-annual variations

When studying monthly means, inter-annual variations can be assessed. The monthly means of UVR, R_g and total ozone were calculated (Figs. 11–14). Due to Sodankylä's high latitude location, the annual variation in solar radiation reaching the ground there is high. As the solar radiation is near zero during the winter months, the influence of the summer months is pronounced when calculating annual radiation doses. We found that the monthly means of erythemally-weighted daily doses measured with the NILU-UV radiometer on the roof of the station were four times higher than those measured in the forest; additionally, the inter-annual variations were smoother in the forest (Fig. 15).

At Sodankylä, summer variations in UVR are mostly affected by variations in total ozone and cloudiness (Arola *et al*. 2003, Lindfors *et al*.

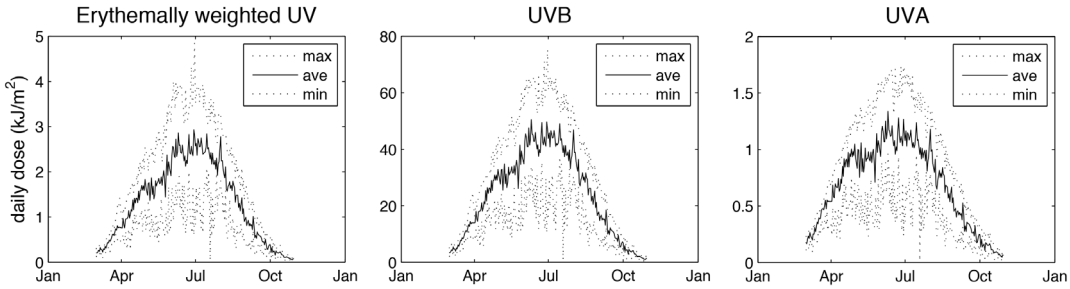

Fig. 10. Average (ave) erythemally-weighted, UVB and UVA daily doses calculated for the period 2002–2012. The maximum (max) and minimum (min) measured daily doses during the time period are also shown. The average daily doses were calculated from the NILU-UV measurements performed on the peatland (prior to 2007) and on the roof of the observatory (after 2007) at Sodankylä.

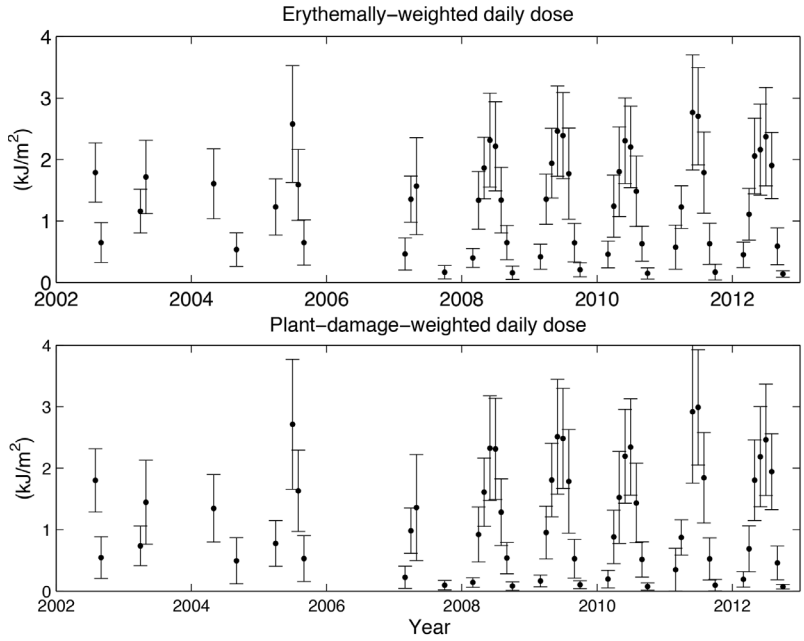

Fig. 11. Monthly means of erythemally-weighted and plant-damage weighted daily doses measured on the peatland (prior to 2007) and on the roof of the observatory (after 2007) at Sodankylä in 2002–2012. One standard deviation limits are also plotted.

2003). Changes in cloudiness can either mask or strengthen the effect of changes in total ozone. Lindfors *et al*. 2007 calculated long-term UV trends based on reconstructed UV radiation doses. The results showed a statistically significant UV increase for the time period 1983–2005 at Sodankylä, dominated by an increase in R_g, i.e., a decrease in cloudiness.

A measurement of R_g can be used to indicate changes in cloudiness, as R_g is mostly attenuated by clouds. The highest summer R_g values were measured in 2002 (May and June) and 2003 (June and July), and indicated summers with low cloudiness. The lowest summer R_g values were measured in June of 2000, 2004 and 2008, and in July of 2001, 2007 and 2010.

The ratio of monthly mean erythemally-weighted and UVA (ERY/UVA) daily doses were calculated for June–August (Fig. 16). As the erythemal action spectrum gives more weight to short UVB wavelengths than UVA wavelengths, the changes in total ozone should be seen as changes in erythemally weighted UV dose rates. In our study, the anti-correlation between total ozone and erythemally-weighted UV dose rates was clearly seen in June, when high and low total ozone values occurred in 2010 and 2011, respectively (Figs. 16 and 17). Our results also

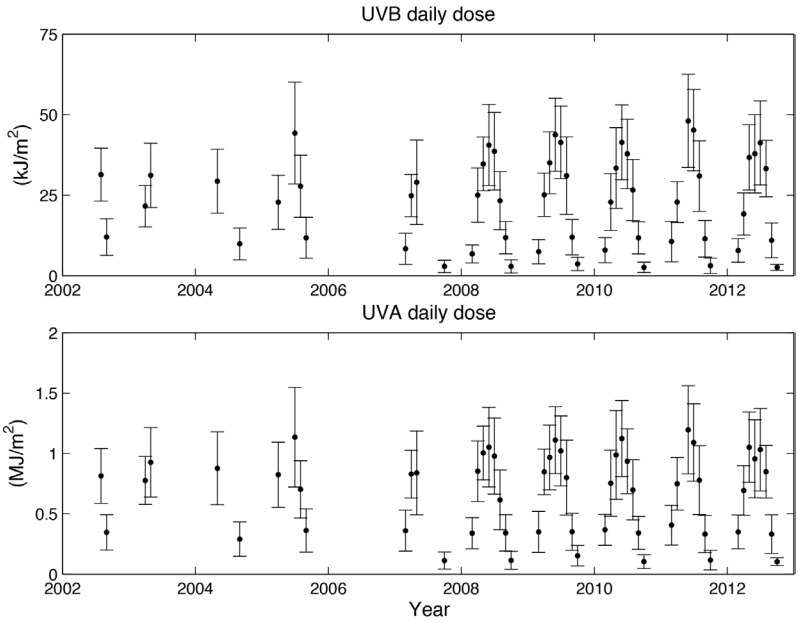

Fig. 12. Monthly means of UVB and UVA daily doses measured on the peatland (prior to 2007) and on the roof of the observatory (after 2007) at Sodankylä in 2002–2012. One standard deviation limits are also plotted.

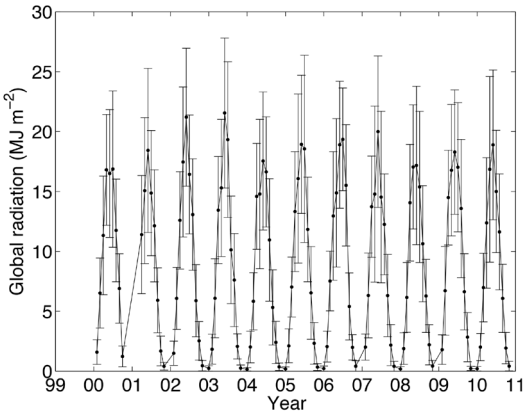

Fig. 13. Monthly means of global radiation daily sums measured on the roof of the observatory at Sodankylä in 2000–2010. One standard deviation limits are also shown.

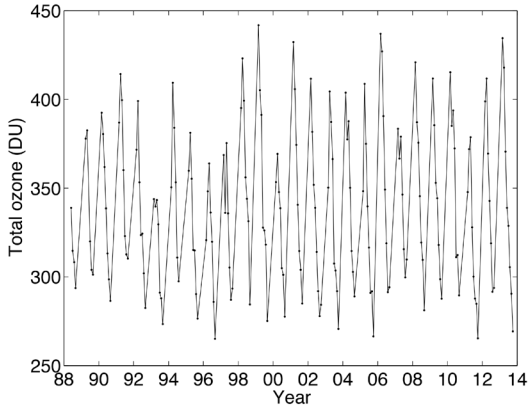

Fig. 14. Monthly mean total ozone measured with the Brewer spectroradiometer in 1988–2013.

confirmed the results of Karpechko *et al*. (2013), where severe stratospheric ozone loss of spring 2011 led to increased UV levels until August.

At Sodankylä, due to the Brewer-Dobson circulation and natural stratospheric ozone destruction under sunlight, the highest total ozone values are measured in spring and the lowest values in late autumn. The lowest monthly mean of 265 DU was measured in September 1996 and the highest, 442 DU, in March 1999. When studying the total ozone time series for March, the years 1993–1997, 2000, 2003, 2005 and 2011, when severe springtime Arctic ozone depletion occurred, are clearly seen. The effect is seen as increased UVI in March, when studying time series of the monthly mean daily maximum UV index (Fig. 18). Even though the measured UVI is low in March, mostly below 2, the measured increase in UVI can be more than 80% (Bernhard *et al*. 2013).

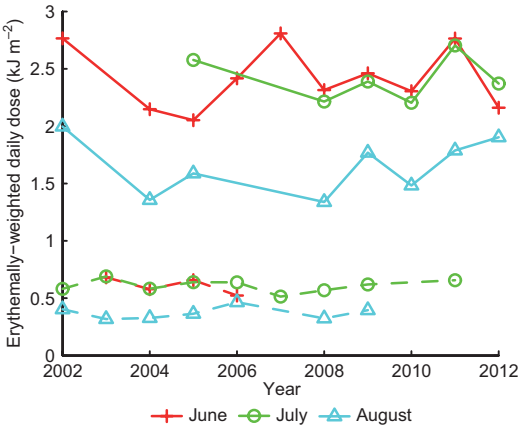

Fig. 15. Monthly means of erythemally-weighted daily doses measured from the roof of the observatory (continuous lines) and in the forest (dashed lines) at Sodankylä in June–August in 2002–2012.

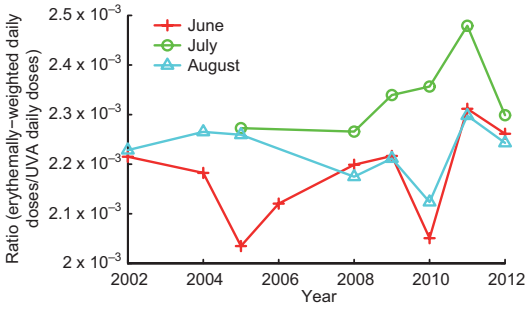

Fig. 16. Ratio of monthly mean erythemally-weighted and UVA (ERY/UVA) daily doses in June–August in 2002–2012.

Conclusions

Here, we studied the time series of UV, global radiation and PAR measured at the Pallas-Sodankylä GAW station of the Finnish Meteorological Institute-Arctic Research Centre. We scaled the multifilter measurements to the spectroradiometer measurements and found an agreement of 5% for erythemally-weighted and UVB dose rates. UV measurements were performed in a coniferous forest, from the roof of the station, and at a field site in a peatland. The UVB and UVA doses in the forest were on average about 25% of those measured in the nearby open area.

In order to study UV daily doses, use was made of the NILU-UV radiometer measurements during the period 2002–2012. The maximum measured UVB and UVA daily doses were 75.0 kJ m^{-2} (in June 2011) and 1.74 MJ m^{-2} (in June 2009), respectively. The ratio of erythemally-weighted UV and UVA daily doses were calculated in order to find the years, in which total ozone was the driving factor contributing to

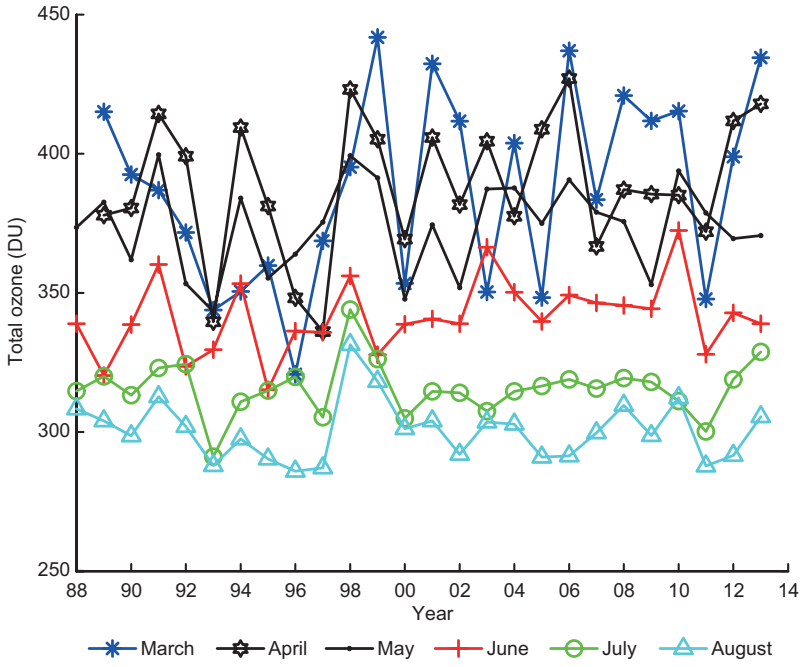

Fig. 17. Monthly mean total ozone in March–August in 1988–2013.

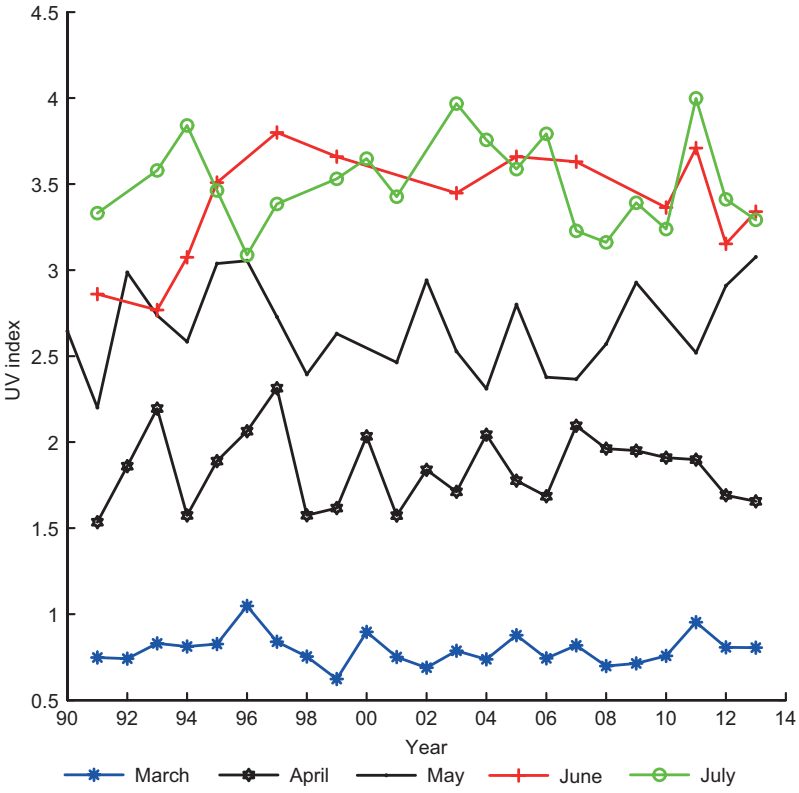

Fig. 18. Monthly means of maximum daily UV indices in March–July in 1990–2013.

UV amounts during summer time. A clear anti-correlation was seen in June of the years 2010 and 2011. The UV index time series were calculated from the Brewer spectroradiometer measurements for the period 1990–2013. A maximum UV index of 6 was measured in 2011 and 2013.

The maximum measured PAR was 1830 μmol m^{-2} s^{-1} in June 2000, while maximum global radiation daily dose was 31.44 MJ m^{-2} in June 2010. In April and May, the highest PAR and global radiation values within the mean diurnal cycles were similar to those in June and July. This may result from a higher ground albedo due to snow in April and May. The influence of snow was also seen as enhanced values in the yearly cycles of UV radiation in April.

Acknowledgements: The Academy of Finland has given support for this work through the SAARA and UTLS (grant number 140408) projects. We are grateful to the operators of the station at Sodankylä for their daily maintenance of the radiation measurements and for performing the lamp calibrations of the Brewer spectroradiometers. We thank Tomi Karppinen for the quality control of Brewer spectroradiometer measurements.

References

Andrady A., Aucamp P.J., Bais, A.F., Ballaré C.L., Björn L.O., Borman J.F., Caldwell M., Cullen A.P., Erickson D.J., De Gruil F.R., Häder D.-F., Ilyas M., G. Kulandaivelu G., Kumar H.D., Longstreth J., McKenzie R.L., Norval M., Paul N., Redhwi H.H., Smith R.C., Salomo K.R., Sulzberger B., Takizawa Y., Tang X., Teramura A.H., Torikai A., Van Der Leun J.C., Wilson S.R., Worrest R.C. & Zepp R. 2009. Environmental effects of ozone depletion and its interactions with climate change: Progress report, 2008. *Photoch. Photobio. Sci.* 8: 13–22.

Arola A., Lakkala K., Bais A., Kaurola J., Meleti C. & Taalas P. 2003. Factors affecting short- and long-term changes of spectral UV irradiance at two European stations. *J. Geophys. Res.* 108, 4549, doi:10.1029/2003JD003447.

Bais A., Zerefos C. & McElroy C.T. 1996. Solar UVB measurements with the double- and single-monochromator Brewer Ozone Spectrophotometers. *Geophys. Res. Lett.* 23: 833–836.

Bernhard G., Dahlback A., Fioletov V., Heikkilä A., Johnsen B., Koskela T., Lakkala K. & Svendby T.M. 2013. High levels of ultraviolet radiation observed by ground-based instruments below the 2011 Arctic ozone hole. *Atmos. Chem. Phys.* 13: 10573–10590.

Caldwell M., Camp L., Warner C. & Flint S.D. 1986. Action spectra and their key role in assessing biological consequences of solar UV-B radiation change. In: Wor-

rest R.C. & Caldwell M.M. (eds.), *Stratospheric ozone reduction, solar ultraviolet radiation and plant life*, Springler-Verlag, Berlin, pp. 87–111.

Dahlback A. 1996. Measurements of biologically effective UV doses, total ozone abundances, and cloud effects with multichannel, moderate bandwidth filter instruments. *Appl. Opt.* 35: 6514–6521.

Diaz S., Booth C.R., Armstrong R., Brunat C., Cabrera S., Camiliân C., Casiccia C., Deferrari G., Fuenzalida H., Lovengreen C., Paladini A., Pedroni J., Rosales A., Zagareses H. & Vernet M. 2005. Multichannel radiometer calibration: a new approach. *Appl. Opt.* 44: 5374–5380.

Eyring E.A., Arblaster J.M., Cionni I., Sedlácek J., Perlwitz J., Young P.J., Bekki S., BeRgmann D., Cameron-Smith P., Collins W.J., Faluvegi G., Gottschaldt K.-D., Horowitz L.W., Kinnison D.E., Lamarque J.-F., Marsh D.R., Saint-Martin D., Shindell D.T., Sudo K., Szopa S. & Watanabe S. 2013. Long-term ozone changes and associated climate impacts in CMIP5 simulations. *J. Geophys. Res.* 118: 5029–5060.

Farman J., Gardiner B. & Shanklin J. 1985. Large losses of total ozone in Antarctica reveal seasonal CLO_x/NO_x interaction. *Nature* 315: 207–210.

Fountoulakis I., Bais A.F., Tourpali K., Fragkos K. & Misios S. 2014. Projected changes in solar UV radiation in the Arctic and sub-Arctic Oceans: effects from changes in reflectivity, ice transmittance, clouds, and ozone. *J. Geophys. Res.* 119: 8073–8090.

Garane K., Bais A.F., Kazadzis S., Kazantzidis A. & Meleti C. 2006. Monitoring of UV spectral irradiance at Thessaloniki (1990–2005): data re-evaluation and quality control. *Ann. Geophys.* 24: 3215–3228.

Gröbner J. & Sperfeld P. 2005. Direct traceability of the portable QASUME irradiance standard of the PTB. *Metrologia*. 42: 134–139.

Høiskar B., Haugen R., Danielsen T., Kylling A., Edvardsen K., Dahlback A., Johnsen B., Blumthaler M. & Schreder J. 2003. Multichannel moderate-bandwidth filter instrument for measurement of the ozone-column amount, cloud transmittance, and ultraviolet dose rates. *Appl. Optics*. 42: 3472–3479.

IPCC 2013. *Climate change 2013: the physical science basis*. Contribution of Working Group I to the Fifth Assessment Report of the Intergovernmental Panel on Climate Change, Cambridge University Press, Cambridge, United Kingdom and New York, NY, USA.

Johnsen B., Mikkelborg O., Hannevik M., Nilsen L., Saxebøl G. & Blaasaas K. 2002. *The Norwegian UV-monitoring program Period 1995/96 to 2001*. Strålevern Rapport 2002:4, Norwegian Radiation Protection Authority, Østerås.

Karpechko A.Y., Backman L., Thölix L., Ialongo I., Andersson M., Fioletov V., Heikkilä A., Johnsen B., Koskela T., Kyrölä E., Lakkala K., Myhre C.L., Rex M., Sofieva V., Tamminen J. & Wohltmann I. 2013. The link between springtime total ozone and summer UV radiation in northern hemisphere extratropics. *J. Geophys. Res.* 118: 8649–8661.

Karppinen T., Redondas A., Garca R., Lakkala K., McElroy C.T. & Kyrö E. 2014: Compensating for the effects of stray light in single monochromator Brewer spectrophotometer ozone retrieval. *Atmosphere–Ocean* 01/2014, doi:10.1080/07055900.2013.871499.

Kivi R., Kyrö E., Turunen T., Ulich T. & Turunen E. 1999. Atmospheric trends above Finland: II. Troposphere and stratosphere. *Geophysica* 35: 71–85.

Kivi R., Kyrö E., Turunen T., Harris N., von der Gathen P., Rex M., Andersen S.B. & Wohltmann I. 2007. Ozonesonde observations in the Arctic during 1989–2003: Ozone variability and trends in the lower stratosphere and free troposphere. *J. Geophys. Res.* 112, D08306, doi:10.1029/2006JD007271.

Kratzenberg M.G., Beyer H.G., Colle S. & Albetayz A. 2006. Uncertainty calculations in pyranometer measurements and application. In: *ASME 2006 International Solar Energy Conference (ISEC2006), July 8–13, Denver, Colorado, U.S.A.*, paper ISEC2006-99168, pp. 689–698, doi:10.1115/ISEC2006-99168.

Kübarsepp T., Kärhä P., Manoocheri F., Nevas S., Ylianttila L. & Ikonen E. 2000. Spectral irradiance measurements of tungsten lamps with filter radiometers in the spectral range 290 nm to 900 nm. *Metrologia*. 37: 305–312.

Kyrö E., Taalas P., Jörgensen T., Knudsen B., Stordal F., Braahten G., Dahlback A., Neuber B., Krüger R., Dorokhov V., Yushkov V., Rudakov V. & Torres A. 1992. Analysis of the ozone soundings made during the first quarter of 1989 in the Arctic. *J. Geophys. Res.* 97: 8083–8091.

Lakkala K., Kyrö E. & Turunen T. 2003. Spectral UV measurements at Sodankylä during 1990–2001. *J. Geophys. Res.* 108, 4621, doi:10.1029/2002JD003300.

Lakkala K., Arola A., Heikkilä A., Kaurola J., Koskela T., Kyrö E., Lindfors A., Meinander O., Tanskanen A., Gröbner J. & Hülsen G. 2008. Quality assurance of the Brewer UV measurements in Finland. *Atmos. Chem. Phys.* 8: 3369–3383.

Lakkala K., Redondas A., Meinander O., Torres C., Koskela T., Cuevas E., Taalas P., Dahlback A., Deferrari G., Edvardsen K. & Ochoa H. 2005. Quality assurance of the solar UV network in the Antarctic. *J. Geophys. Res.* 110, D15101, doi:10.1029/2004JD005584.

Lindfors A., Arola A., Kaurola J., Taalas P. & Svenøe T. 2003. Long-term erythemal UV doses at Sodankylä estimated using total ozone, sunshine duration, and snow depth. *J. Geophys. Res.* 108, 4518, doi:10.1029/2002JD003325.

Lindfors A., Kaurola J., Arola A., Koskela T., Lakkala K., Josefsson W., Olseth J.A. & Johnsen B. 2007. A method for reconstruction of past UV radiation based on radiative transfer modeling: applied to four stations in northern Europe. *J. Geophys. Res.* 112, D23201, doi:10.1029/2007JD008454.

Manney G., Santee M.L., Rex M., Livesey N.J., Pitts M.C., Veefkind P., Nash E.R., Wohltmann I., Lehmann R., Froidevaux L., Poole L.R., Schoeberl M.R., Haffner D.P., Davies J., Dorokhov V., Gernandt H., Johnson B., Kivi R., Kyrö E., Larsen N., Levelt P.F., Makshtas A., McElroy T., Nakajima H., Parrondo M., Tarasick D.W., Von der Gathen P., Walker K.A. & Zinoviev N.S. 2011. Unprecedented Arctic ozone loss in 2011. *Nature* 478: 469–475.

McKinlay A. & Diffey B., 1987: A reference action spectrum for ultraviolet induced erythema in human skin. In: Passchler W.R. & Bosnakovic B.F.M. (eds.), *Human exposure to ultraviolet radiation: risks and regulations. Proceedings of Seminar Held in Amsterdam, 23–25 March 1987*, Elsevier, Amsterdam, pp. 83–87.

Meinander O., Kontu A., Lakkala K., Heikkilä A., Yliant-tila L. & Toikka M. 2008. Diurnal variations in the UV albedo of Artcic snow. *Atmos. Chem. Phys.* 8: 6551–6563.

Thum T., Aalto T., Laurila T., Aurela M., Kolari P. & Hari P. 2007. Parametrization of two photosynthesis models at the canopy scale in a northern boreal Scots pine forest. *Tellus* 59B: 874–890.

Von der Gathen P., Rex M., Harris N.R.P., Lucic D., Knudsen B.M., Braathen G.O., de Backer H., Fabian R., Fast H., Gil M., Kyrö E., Mikkelsen I.S., Rummukainen M., Staehelin J. & Varotsos C. 1995. Observational evidence for chemical ozone depletion over the Arctic in winter 1991–92. *Nature* 375: 131–134.

Wang K., Augustine J. & Dickinson R.E. 2012. Critical assessment of surface incident solar radiation observations collected by SURFRAD, USCRN and AmeriFlux networks from 1995 to 2011. *J. Geophys. Res.* 117, D23105, doi: 10.1029/2012jd017945.

WMO 1997. *Report of the WMO-WHO meeting of experts on standardizations of UV indices and their dissemination to the public*. World Meteorological Organization (WMO), Global Atmosphere Watch, Report no. 127, Geneva, Switzerland.

WMO 2011. *Scientific assessment of ozone depletion: 2010*. World Meteorological Organization (WMO), Global Ozone Research and Monitoring Project, Report no. 52, Geneva, Switzerland.

WMO 2014. *Assessment for decision makers: Scientific assessment of ozone depletion: 2014*. World Meteorological Organization, Global Ozone Research and Monitoring Project, Report no. 56, Geneva, Switzerland.

Young A., Björn L., Moan J. & Nultsch W. 1993. *Environmental UV photobiology*. Plenum Press, New York.